Non–Birkhoff Periodic Orbits in a Circle Mapping

Yoshihiro YAMAGUCHI[1] and Kiyotaka TANIKAWA[2]

[1] Teikyo Heisei University, Ichihara, Chiba 290-0193, Japan.

[2] National Astronomical Observatory, Mitaka, Tokyo 181-8588, Japan.

(Received)

Abstract

Birkhoff and Non–Birkhoff types of periodic orbits are defined in circle mappings. The dynamical order relation of non–Birkhoff periodic orbits (NBOs) with period longer than equal 3 is proved. The braids are constructed for NBOs and the topological entropy is estimated.

1 Introduction

Dynamics of one dimensional circle mapping offer useful information on periodic orbits, quasi-periodic and chaotic motions.[1−3] In many cases, systems with one external parameter have been the target of research. The parameter region pertaining to the local motion[4] or to the Arnold tongues[3] has been investigated. Properties of systems in the parameter region where local and global motions mix are not made clear. By the global motion, we mean that of revolving the circle. In this situation, the mixing of the local and global motions (this will be called the mixed state) induces complicated phenomena. In this paper, we pay attention to the appearance of periodic orbits (called windows in the bifurcation diagram) in the parameter region of mixed state, and try to estimate the topological entropy of complicated motions.

We consider C^0 mapping f on circle $\mathbf{S}^1$ defined by

$$\theta_{n+1} = f(\theta_n) \text{ (Mod 1)}, \tag{1}$$

where $f(\theta)$ is assumed to satisfy the following conditions.
[1] $f(\theta+1) = f(\theta)+1$,
[2] $f(\theta)$ has one local maximum point at $\theta_{max} \in (0, \theta_c)$ and has one local minimum point at $\theta_{min} \in (\theta_c, 1)$ for some $0 < \theta_c < 1$.
[3] There exist two fixed points θ_l and θ_r satisfying $\theta_c < \theta_l < \theta_r < 1$. Note that θ_r is an unstable fixed point.

Since we discuss periodic orbits revolving the circle, we work in universal cover $\mathbf{R}^1$ of $\mathbf{S}^1$. In $\mathbf{R}^1$, we use a lift $\hat{f} : \mathbf{R}^1 \to \mathbf{R}^1$ of $f : \mathbf{S}^1 \to \mathbf{S}^1$. The lift $\hat{f}$ is chosen to keep the fixed points for f fixed, so it is uniquely defined.

We address the following questions on the circle mappings satisfying [1] – [3], and answer partially to them. What periodic orbits exist in the mixed state, and what types of dynamical order relation between them hold? What is the topological entropy in the system? We use, in obtaining periodic orbits, the standard tools in the one-dimensional mappings such as primitive mappings, covering relations, oriented graphs and so on. Construction of braids and estimation of topological entropy follow those of our preceding articles.[12),13),14)]

In §2, we introduce several definitions and notation, and prove the dynamical order relation for non–Birkhoff type periodic orbits (NBOs) . In §3, the braids for NBOs are constructed, and the topological entropy is estimated. In §4, we give several remarks.

2 Dynamical order relation

2.1 Definition and notation

Birkhoffness or non–Birkhoffness of periodic orbits has been introduced in two–dimensional twist mappings.[5)] The notion is most relevant to circle mappings. A point $\hat{\theta} \in \mathbf{R}^1$ is called a p/q-periodic point for $\hat{f}$ if

$$\hat{f}^q(\hat{\theta}) = \hat{\theta} + p. \tag{2}$$

The orbit of $\hat{\theta}$ is $O(\hat{\theta}) = \{\cdots, \hat{f}^{-1}(\hat{\theta}), \hat{\theta}, \hat{f}(\hat{\theta}), \cdots\}$. The extended orbit of $\hat{\theta}$ is

$$EO(\hat{\theta}) = \{\hat{f}^k(\hat{\theta}) + m : k, m \in \mathbf{Z}\}. \tag{3}$$

A p/q-periodic point $\hat{\theta}$ is called Birkhoff if for any $\hat{r}, \hat{s} \in EO(\hat{\theta})$

$$\hat{r} < \hat{s} \;\Rightarrow\; \hat{f}(\hat{r}) < \hat{f}(\hat{s}). \tag{4}$$

If the extended orbit of a periodic point has a couple of points not satisfying Eq.(4), we call it the non–Birkhoff periodic point and its orbit the non-Birkhoff periodic orbit (NBO). From now on, we use the convention $\hat{\theta}_k = \hat{f}^k(\hat{\theta}_0)$.

Let us consider a p/q–periodic orbit $O(\hat{\theta}_0)$. If $\hat{\theta}_k > \hat{\theta}_{k-1}$ and $\hat{\theta}_k > \hat{\theta}_{k+1}$ hold at some k $(1 \le k < q)$, $\hat{\theta}_k$ is called a turning-back point. If $\hat{\theta}_{k'} < \hat{\theta}_{k'-1}$ and $\hat{\theta}_{k'} < \hat{\theta}_{k'+1}$ hold at some k' $(0 \le k' < q)$, $\hat{\theta}_{k'}$ is called a turning-forward point. We call these the *turning points*. In this paper, we consider NBOs with turning points. Note that there are NBOs with no turning points.[12)] We can choose $\hat{\theta}_0$ as a starting point of the orbit so that $\hat{\theta}_1$ be the first turning-back point. Let $\hat{\theta}_{k_a+1}$ $(k_a \ge 1)$ be the first turning-forward point, and $\hat{\theta}_{k_b+1}$ $(k_b \ge 1)$ be the last turning-forward point. If the orbit has only two turning points, then $k_a = k_b$. We restrict our attention to NBOs satisfying the condition

$$\hat{\theta}_0 < \hat{\theta}_{k_b+1} \le \hat{\theta}_{k_a+1} < \hat{\theta}_1. \tag{5}$$

Later, we categorize NBOs with $2n$ $(n \ge 1)$ turning points by k_a and the number of turning points.

If a closed interval $I \subset \mathbf{R}^1$ contains one turning point, we denote it by $\tilde{I}$. Let I_1 and I_2 be two closed intervals satisfying $\mathrm{Int}(I_1) \cap \mathrm{Int}(I_2) = \emptyset$ where $\mathrm{Int}(I)$ is the interior of I. If the relation $I_2 \subset \hat{f}(I_1)$ holds, we write $I_1 \succ I_2$, and we say I_1 covers I_2. We also call $I_1 \succ I_2$ the oriented graph of intervals, or the covering relation.

The rotation number ν of an orbit of $\hat{\theta} \in \mathbf{R}$ is defined by

$$\nu = \lim_{n\to\infty} \sup \frac{\hat{f}^n(\hat{\theta}) - \hat{\theta}}{n}. \tag{6}$$

A $1/q$–NBO with k_a and two turning points is denoted by

$$\left(\frac{1}{q}\right)^2_{k_a}. \tag{7}$$

If the existence of a $1/q$–NBO with k_a and two turning points implies the existence of a $1/q'$–NBO with k'_a and two turning points, then we write as

$$\left(\frac{1}{q}\right)^2_{k_a} \to \left(\frac{1}{q'}\right)^2_{k'_a}, \tag{8}$$

and we simply say that $(1/q)^2_{k_a}$ implies $(1/q')^2_{k'_a}$. We also say that $(1/q')^2_{k'_a}$ is dominated by $(1/q)^2_{k_a}$.

2.2 NBOs with period–3

We assume that there exists a $1/3$–NBO in the universal cover $\mathbf{R}^1$ of $\mathbf{S}^1$ in some parameter set satisfying the orbital order

$$0 \le \hat{\theta}_0 < \hat{\theta}_2 < \hat{\theta}_1 < 1 \le \hat{\theta}_3 = \hat{\theta}_0 + 1, \tag{9}$$

where $\hat{\theta}_i = \hat{f}^i(\hat{\theta}_0)$ and $k_a = k_b = 1$. This orbit is $(1/3)^2_1$ following the convention adopted in §2.1. Since the orbit turns back at $\hat{\theta}_1$, we have $\hat{\theta}_l < \hat{\theta}_1 < \hat{\theta}_r$. We define four intervals:

$$\begin{aligned} I_1 &= [0, \hat{\theta}_{\max}], & (10)\\ I_2 &= [\hat{\theta}_{\max}, \hat{\theta}_{\min}], & (11)\\ I_3 &= [\hat{\theta}_{\min}, 1], & (12)\\ SI_1 &= [1, \hat{\theta}_{\min} + 1]. & (13) \end{aligned}$$

One observes that a $(1/3)^2_1$ exists if the covering relation

$$I_1 \succ \tilde{I}_3 \succ \tilde{I}_2 \succ SI_1 \tag{14}$$

holds. In order to guarantee (14), we use three conditions.

$$\begin{aligned} \hat{f}(0) &\le \hat{\theta}_{\min}, & (15)\\ \hat{f}(\hat{\theta}_{\min}) &\le \hat{\theta}_{\max}, & (16)\\ \hat{f}(\hat{\theta}_{\max}) &\ge 1 + \hat{\theta}_{\max}. & (17) \end{aligned}$$

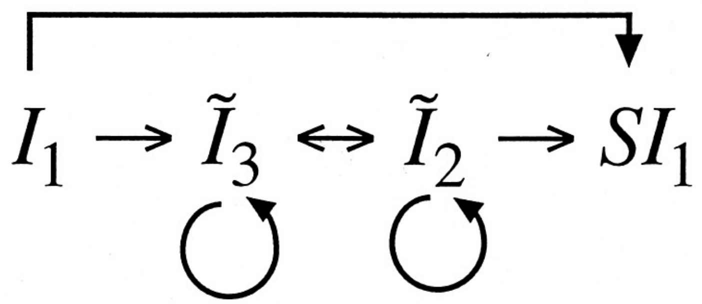

Fig. 1. The oriented graph of the intervals.

Equations (15)–(17) give an oriented graph of intervals shown in Fig. 1. This graph contains the covering relation (14) as a subgraph. Analysis of Fig. (1) gives Proposition 1.

Proposition 1. $(1/3)_1^2$ implies $1/n$–NBOs ($n \geq 4$).

Proof. A cycle $I_1 \succ \tilde{I}_3 \succ I_3 \succ \tilde{I}_2 \succ SI_1$ gives a 1/4–NBO. Similarly, we can construct a cycle with period longer than 4. (Q.E.D.)

2.3 Theorem

In this section, we elaborate the appearance order or the dynamical order of NBOs found in Proposition 1.

Lemma 1. For $1/q$–NBOs with $q \geq 3$, $k_a(\geq 1)$ and with two turning points for the circle mapping f satisfying [1]-[3], the following dynamical order relation holds.

$$\begin{array}{ccccccccc}
(1/3)_1^2 & \rightarrow & (1/4)_1^2 & \rightarrow & (1/5)_1^2 & \rightarrow & (1/6)_1^2 & \rightarrow \cdots \\
\downarrow & & \downarrow & & \downarrow & & \downarrow & \\
(1/5)_2^2 & \rightarrow & (1/6)_2^2 & \rightarrow & (1/7)_2^2 & \rightarrow & (1/8)_2^2 & \rightarrow \cdots \\
\downarrow & & \downarrow & & \downarrow & & \downarrow & \\
(1/7)_3^2 & \rightarrow & (1/8)_3^2 & \rightarrow & (1/9)_3^2 & \rightarrow & (1/10)_3^2 & \rightarrow \cdots \\
\downarrow & & \downarrow & & \downarrow & & \downarrow & \\
\vdots & & \vdots & & \vdots & & \vdots &
\end{array}$$

Remarks. We will use the matrix notation to specify the position of NBOs in Lemma 1. Regarding the above table as a matrix, we take $(1/(2i+j))_i^2$ as the (i,j) $(i,j \geq 1)$ element. Thus, for example, we say $(1,1) \rightarrow (1,2)$ if the forcing relation $(1/3)_1^2 \rightarrow (1/4)_1^2$ holds.

Proof: In order to prove Lemma 1, we use *the primitive tight mapping*[2),6),7)] which is the simplest piecewise linear mapping having a periodic orbit with the given orbital order. Using the information of the NBO defined by Eq. (9), we can construct the primitive tight mapping $\hat{F}$, shown in Fig. 2. In the figure, the relation $SI_i = I_i + 3$ holds and the orbital order of the period–3 orbit is expressed by $0 \rightarrow 2 \rightarrow 1 \rightarrow 3$. Figure 3 is an oriented graph showing the covering relation between intervals. Each interval I_i in Fig. 2 has a unit length. We can change the length and use another continuous function connecting adjacent two points. However, new oriented graph for such mappings contains Fig. 3 as a subgraph. The oriented graph shown in Fig. 3 implies the existence of a cycle from I_1 to SI_1.

Using the oriented graph, we can determine periodic orbits dominated by $(1/3)_1^2$. The following cycle gives a period–4 orbit.

$$I_1 \succ \tilde{I}_3 \succ \tilde{I}_2 \succ I_3 \succ SI_1. \tag{18}$$

The rotation number of the orbit is 1/4 since $SI_1 \subset \hat{F}^4(I_1)$. The orbit is non-Birkhoff because there are turning points in I_2 and I_3. Obviously we have $k_B = 1$. Then the orbit is $(1/4)_1^2$. Thus $(1,1) \rightarrow (1,2)$ is proved. It is to be noted that the orbital points of $(1/4)_1^2$ are not at the endpoints of intervals since these are points of $(1/3)_1^2$. (This fact is true for cases treated below.)

We have two cycles for period–5 orbit satisfying $SI_1 \subset \hat{F}^5(I_1)$.

$$I_1 \succ \tilde{I}_3 \succ I_2 \succ \tilde{I}_2 \succ I_3 \succ SI_1, \tag{19}$$

$$I_1 \succ \tilde{I}_3 \succ I_3 \succ \tilde{I}_2 \succ I_3 \succ SI_1. \tag{20}$$

These give the same 1/5–NBOs with $k_a = 2$. Thus $(1,1) \to (2,1)$ is proved.

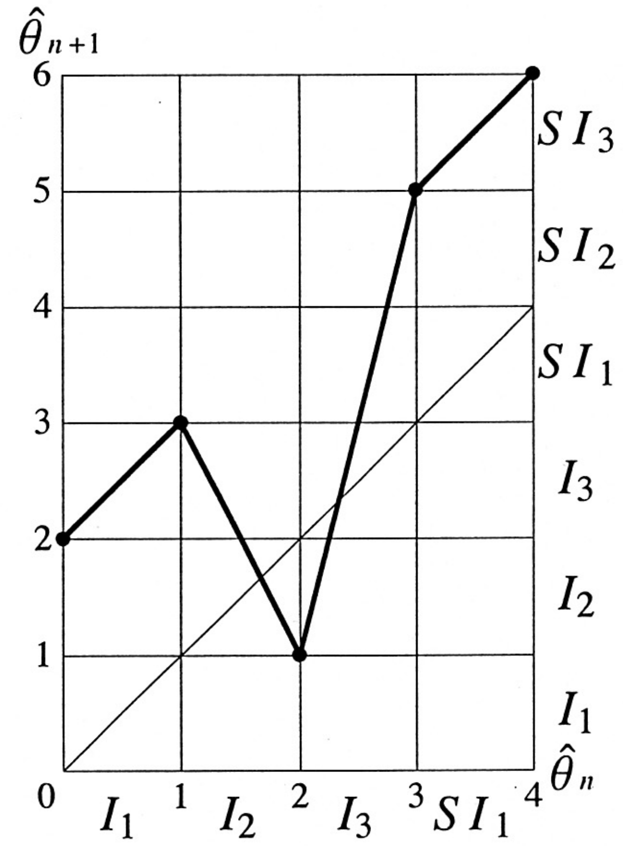

Fig. 2. Primitive tight mapping constructed by $(1/3)^2_1$.

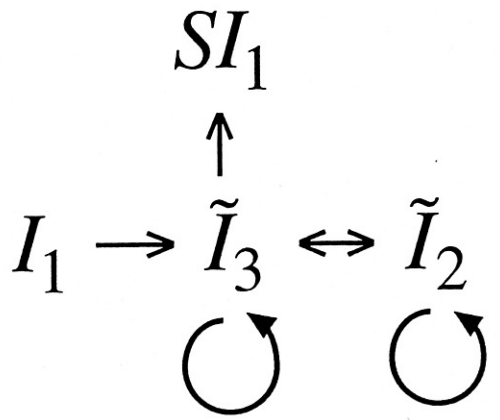

Fig. 3. The oriented graph of the intervals, and the unnecessary arrows are omitted.

Next we prove the general cases of $(i,j) \to (i,j+1)$ and $(i,j) \to (i+1,j)$. The existence of $(1/(2i+j))^2_i$ gives the primitive tight mapping shown in Fig. 4, in which

$\hat{F}(I_1^l) = I_{i+2}^l$ and $I_{i+2}^r \subset \hat{F}(I_2^l)$ hold. The relation between the intervals is displayed in Fig. 5, where unnecessary arrows are omitted. We want to find the cycle from I_1^l to SI_1^l. The shortest orbit has a period $(2i+j+1)$ and $k_i = i$. Thus the relation $(i,j) \to (i,j+1)$ is proved. There are two ways to construct an orbit with period $(2i+j+2)$ and $k_B = i+1$. If we use I_{i+2}^l twice, then we have $I_1^l \succ \tilde{I}_{i+2}^l \succ I_{i+2}^l \succ I_{i+1} \succ \cdots \succ SI_1^l$. If we use I_2 twice, we have $I_1^l \succ \cdots \succ I_3 \succ I_2 \succ \tilde{I}_2 \succ \cdots \succ SI_1^l$. These orbits are expressed by $(1/(2i+j+2))_{i+1}^2$. As a result, $(i,j) \to (i+1,j)$ is proved. The proof completes. Q.E.D.

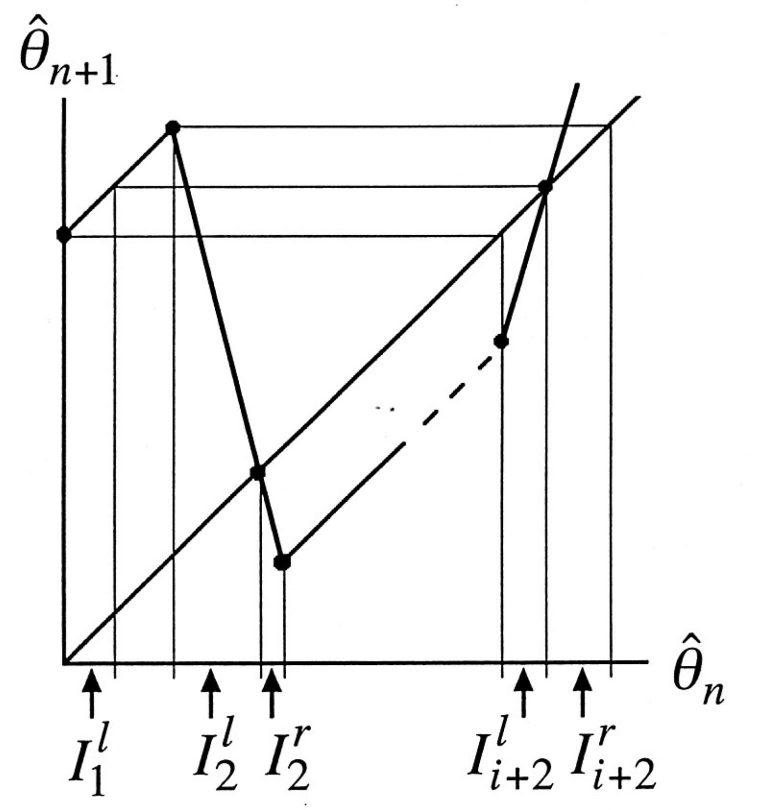

Fig. 4. Primitive tight mapping constructed by $(1/(2i+j))_i^2$ where $I_2 = I_2^l \cup I_2^r$ and $I_{i+2} = I_{i+2}^l \cup I_{i+2}^r$.

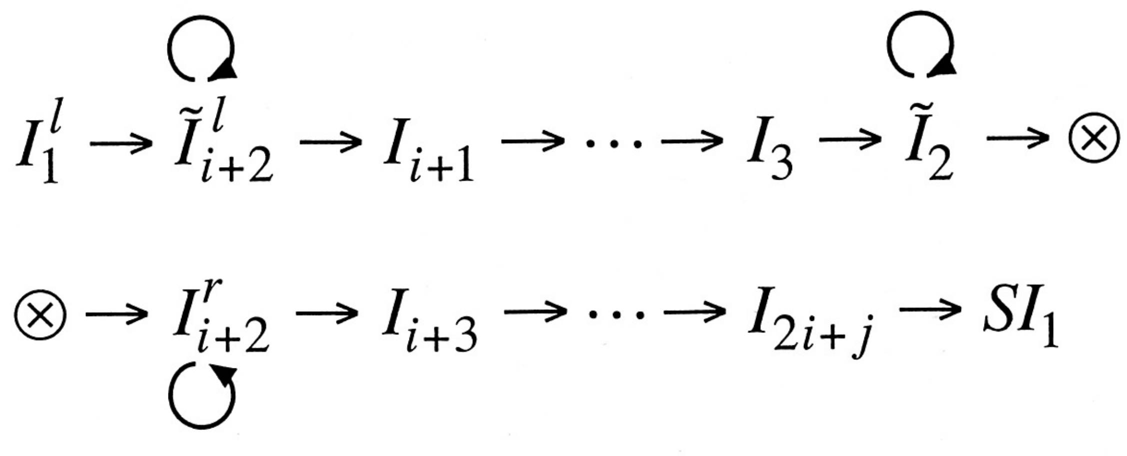

Fig. 5 The oriented graph of the intervals, and the unnecessary arrows are omitted.

We have two ways to obtain NBOs of higher periods. One observes this by looking at Fig.5 carefully. For example, the cycle

$$I_1 \succ \tilde{I}^l_{i+2} \succ \cdots \succ I_3 \succ \tilde{I}_2 \succ \tilde{I}_2 \succ \tilde{I}_2 \succ I^r_{i+2} \succ \cdots \succ SI_1 \tag{21}$$

constructed by using the oriented graph shown in Fig. 5 gives an NBO with four turning points, $k_a = i$ and $k_b = i + 2$. Using I_2 repeatedly, we can prove the existence of NBOs with $2n$ $(n \geq 2)$ turning points. Next using I^l_{i+2} or I^r_{i+2}, we construct cycles of longer periods without increasing the number of turning points. This property comes from the fact that either of I_2 and I_{i+2} contains a fixed point.

In the oriented graph constructed by the primitive tight mapping for $(1/q)^{2n}_{k_a}$, the shortest cycle of an NBO from I_1 to SI_1 with $2n$ turning points not using the edgepoints is $(q+1)$. In fact, the orbit of $(1/q)^{2n}_{k_a}$ passes one edgepoint of I_{i+2}, and the cycle not using edgepoints passes I_{i+2} twice such that it passes I^l_{i+2} to turn back and I^r_{i+2} to go out from the localized region. If we increase the number of turning points by 2, the period of a new cycle increases by 3. Summarizing these facts, we have Lemma 2.

Lemma 2. For $i \geq 1$ and $j \geq 1$, the forcing relations hold.

$$\left(\frac{1}{2i+j}\right)^2_i \to \left(\frac{1}{2i+j+3}\right)^4_i \to \left(\frac{1}{2i+j+6}\right)^6_i \to \cdots . \tag{22}$$

Here we construct the order relation of NBOs with $2m$ $(m \geq 1)$ turning points.

Lemma 3. For NBOs with $\nu = 1/q$ $(q \geq 3)$, k_a (≥ 1) and $2m$ turning points in the circle mapping f satisfying [1]-[3], the following dynamical order relation holds.

$$\begin{array}{ccccccc}
(1/(3m))^{2m}_1 & \to & (1/(3m+1))^{2m}_1 & \to & (1/(3m+2))^{2m}_1 & \to \cdots \\
\downarrow & & \downarrow & & \downarrow & \\
(1/(3m+2))^{2m}_2 & \to & (1/(3m+3))^{2m}_2 & \to & (1/(3m+4))^{2m}_2 & \to \cdots \\
\downarrow & & \downarrow & & \downarrow & \\
(1/(3m+4))^{2m}_3 & \to & (1/(3m+5))^{2m}_3 & \to & (1/(3m+6))^{2m}_3 & \to \cdots \\
\downarrow & & \downarrow & & \downarrow & \\
\vdots & & \vdots & & \vdots &
\end{array}$$

Proof. The proof is similar to that of Lemma 1, and thus is omitted.(Q.E.D.)

From now on, the dynamical ordering in Lemma 3 will be called the dynamical ordering on the m-th floor. m is the number of turning-back or equivalently turning-forward points in an orbit. Consequently, the dynamical ordering on the m-th floor is that for orbits with $2m$ turning points. Using Lemma 2, we can construct the dynamical ordering between the orderings on adjacent two floors. We introduce three dimensional notation (i, j, m), and specify the position of NBOs, for example, $(1/(3m))^{2m}$ at $(1, 1, m)$, $(1/(3m+1))^{2m}_1$ at $(1, 2, m)$ and $(1/(3m+2))^{2m}_2$ at $(2, 1, m)$. As a result, we have theorem 1 on the three dimensional dynamical ordering for NBOs.

Theorem 1. The following dynamical orderings for NBOs hold.

$$\begin{aligned}(i,j,m) &\rightarrow (i,j+1,m), & (23)\\ (i,j,m) &\rightarrow (i+1,j,m), & (24)\\ (i,j,m) &\rightarrow (i,j,m+1), & (25)\end{aligned}$$

where $i,j,m \geq 1$ and an NBO of (i,j,m) element has a rotation number $\nu = 1/(2i+j+3(m-1))$.

2.4 Existence of BOs and their dynamical ordering

According to a theorem by Boyland,[6),7)] if a $1/n$–NBO exists, then there is a rotation band defined by $[0/1, 1/(n-1)]$, and there exists a BO with a rotation number in the rotation band. Combining our results and this theorem, we have Proposition 2.

Proposition 2. A $1/n$–NBO $(n \geq 3)$ implies a $1/(n-1)$–BO.

Let us denote a $1/q$–Birkhoff periodic orbit $(q \geq 2)$ by $(1/q)_B$. There exist q points in the region $[0,\theta_l) \cup (\theta_r, 1) \in \mathbf{S}^1$. Using this fact and the condition [3] of f, we can determine the dynamical order relation of them.

Proposition 3. The following dynamical ordering for BOs holds.

$$(1/2)_B \rightarrow (1/3)_B \rightarrow (1/4)_B \rightarrow \cdots.$$

Proof. We prove the relation $(1/2)_B \rightarrow (1/3)_B$. The others are similarly proved and then the proof is omitted. The primitive tight mapping allowing $(1/2)_B$ is displayed in Fig. 6 where two fixed points are located in I_2 due to [3] and this interval is divided into I_2^l and I_2^r. The oriented graph is obtained in Fig. 7. The existence of loop $I_2^l \succ I_2^l$ depends on the parameters and thus this loop is omitted. There exist two cycles not containing turning points $I_1 \succ I_2^l \succ I_2^r \succ SI_1$ and $I_1 \succ I_2^r \succ I_2^r \succ SI_1$. This implies $(1/3)_B$.(Q.E.D.)

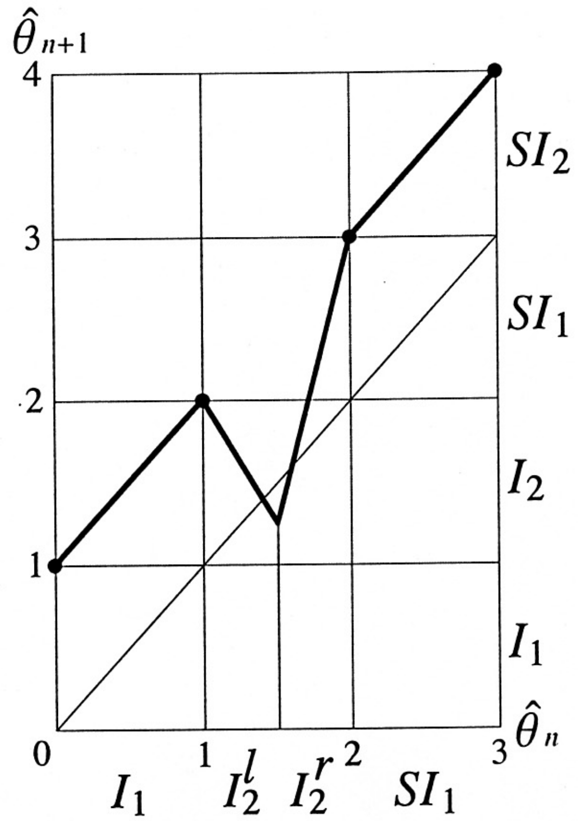

Fig. 6. Primitive tight mapping allowing $(1/2)_B$.

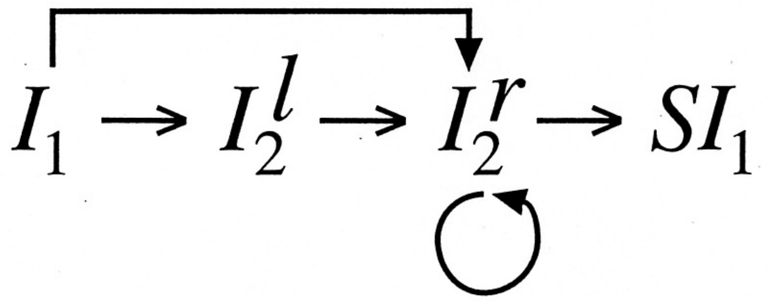

Fig. 7. The oriented graph of intervals constructed by using Fig. 6.

3 Braid and topological entropy

3.1 Braid

We construct braids from periodic orbits by using information on the order of orbital points.[6–8,12] From now on, we use NBOs in the first floor $(i, j, 1)$. The periodic points are located in the circle. Thus we connect θ_n and θ_{n+1} by an arrow. Examples are displayed in Fig. 6 where symbol i stands for θ_i. In Fig. 8(a), an arrow from 1 to 2 intersects that from k to $k+1$. In the braid, a string from 1 to 2 does not intersect that from k to $k+1$. This displays a braid for BO. Figs. (b) and (c) correspond to braids for NBOs. In each braid, two strings intersect each other. If the orbit (fast orbit) goes over the slow orbit or the backward orbit, the string of fast orbit passes behind the string of slow orbit or backward orbit. Using this rule, two braids of Figs. (b) and (c) are constructed.

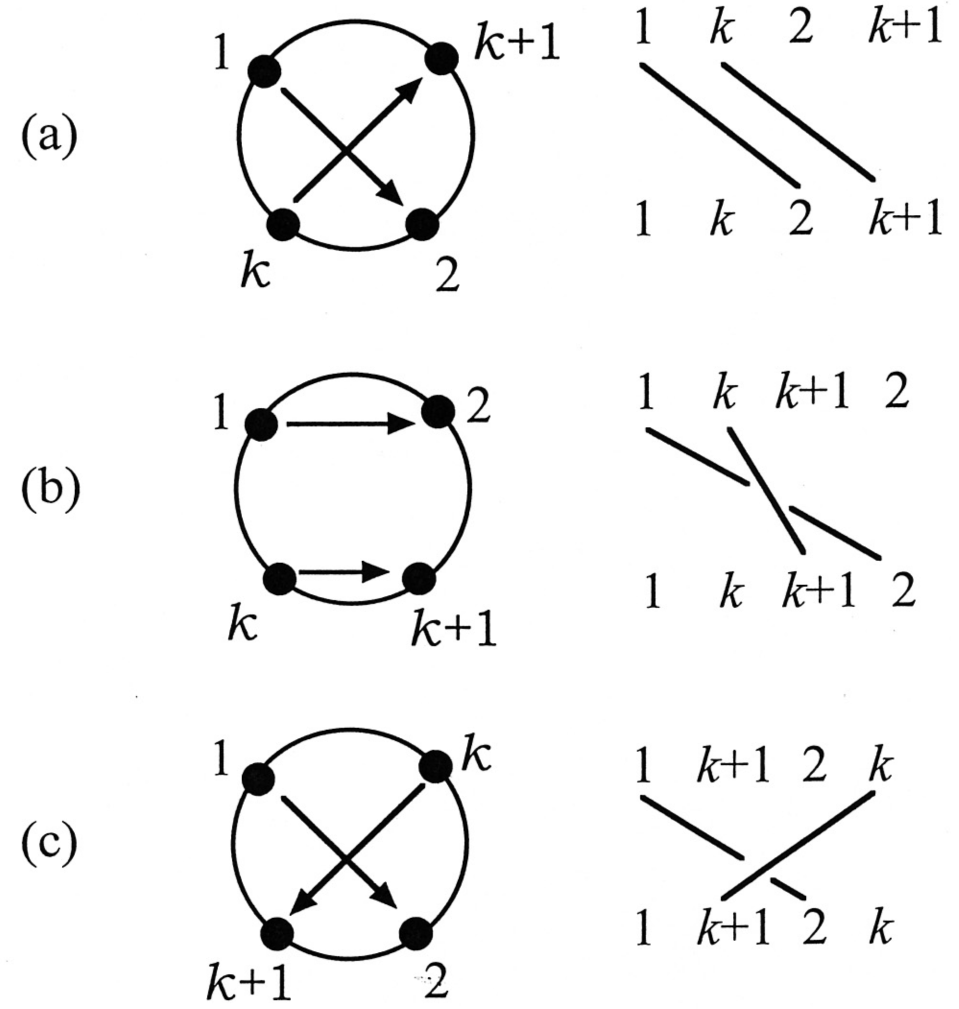

Fig. 8 Fig.(a) shows a part of BO and its braid, and Figs. (b) and (c) display the intersection of braids due to non–Birkhoffness.

We show two braids for 1/5–NBOs expressed by the generator of braid.[11)]

$$\beta(1,3,1) = \sigma_2^{-1}\sigma_1^{-1}\zeta_5 = \sigma_1^{-2}\zeta_5, \tag{26}$$

$$\beta(2,1,1) = \sigma_2^{-1}\sigma_3^{-1}\sigma_1^{-1}\sigma_2^{-1}\zeta_5 = \sigma_1^{-1}\sigma_2^{-1}\sigma_2^{-1}\sigma_1^{-1}\zeta_5 \tag{27}$$

where $\zeta_5 = \sigma_4 \cdots \sigma_1$, and Reidemeister and Markov moves[9] are operated to derive the second expression. The difference of braids comes from that of k_B. We have the braid for an NBO of $(i, j, 1)$ element in Lemma 1.

$$\beta(i, j, 1) = \zeta_{i+1}^{-1} \rho_{i+1}^{-1} \zeta_{2i+j} \tag{28}$$

where $\rho_i = \sigma_1 \cdots \sigma_{i-1}$ and $\zeta_i = \sigma_{i-1} \cdots \sigma_1$. The part ζ_{2i+j} is the braid of 1/5–Birkhoff orbit and the part $\zeta_{i+1}^{-1} \rho_{i+1}^{-1}$ represents the non–Birkhoffness.

3.2 Topological entropy

We show the procedure to estimate the lower bound of topological entropy by using NBOs in Lemma 1. First, we construct the Burau matrix representation[8),9)] corresponding to the braid of an NBO. Next, we calculate the eigenvalues of Burau matrix. The maximum (λ_{max}) of the absolute values of eigenvalues gives the lower bound of topological entropy,[10),11)] expressed by $h = \ln \lambda_{max}$.

Numerical results for topological entropy are shown in Table I. The maximum value is $\ln(\sqrt{5} + 3)/2 = 0.962 \cdots$ estimated by using $(1/3)_1^2$.[8)] The entropy $h(1, j, 1)$ is not a strictly decreasing function of j, but it accumulates at $\ln 2$ in the limit $j \to \infty$. This fact implies that the entropy is larger than $\ln 2$ for finite j. Finally it is noted that we can not determine the forcing relation of NBOs by using the topological entropy estimated in Table I.

Table I: Topological entropy $h(i, j, 1)$ calculated by using the program in Ref. 12).

	$j = 1$	2	3	4	5	6	7
$i = 1$	0.962	0.776	0.767	0.713	0.714	0.694	0.698
2	0.652	0.575	0.558	0.530	0.512	0.508	0.499
3	0.562	0.499	0.491	0.462	0.460	0.445	0.446
4	0.465	0.422	0.416	0.398	0.389	0.382	0.373
5	0.413	0.379	0.375	0.355	0.354	0.342	0.343
6	0.364	0.338	0.334	0.321	0.315	0.310	0.304
7	0.332	0.310	0.307	0.293	0.292	0.282	0.283

4 Remarks

Suppose that f has one bifurcation parameter a, and assume the existence of a critical value a_c such that the mixing of the local and global motions exists at $a > a_c$. The transition from a local state to a mixed state is called the *crisis*. Let $a_c(1/q|_{ka}^2)$ with $q = 2i + j$ be a critical value at which an NBO of $(1/q)_{ka}^2$ appears due to the tangent bifurcation. For BOs, the critical values $a_c(1/q|_B)$ $(q \geq 2)$ are also defined.

In the limit $i \to \infty$, θ_1 tends to θ_r from the left side. In the limit $j \to \infty$, θ_{i+2} tends to θ_r from the right side. The converged situation is that of crisis. We have the relation:

$$\lim_{i \to \infty} a_c(1/q|_i^2) = a_c \text{ for fixed } j, \tag{29}$$

$$\lim_{j \to \infty} a_c(1/q|_i^2) = a_c \text{ for fixed } i, \tag{30}$$

$$\lim_{q \to \infty} a_c(1/q|_B) = a_c^* \tag{31}$$

where a critical value a_c^* is the value for which $f(\theta_{max}) = \theta_r$ holds. The topological entropy is larger than $\ln 2$ at $a > a_c$ since the limiting value is $\ln 2$ for $i = 1$ and $j \to \infty$, and Eqs. (29) and (30) hold.

We have used only the continuity of mapping function to prove Lemmas. Then Theorem 1 holds for a climbing sine–mapping (CSM) defined by

$$f(\theta) = \theta + \frac{K}{2\pi} \sin 2\pi\theta + \Omega, \tag{32}$$

where $K > 0$ and $\Omega \geq 0$. This mapping satisfies the conditions [1]-[3] where $\theta_c = 1/2$. In the case that Ω is fixed, we can regard K as a bifurcation parameter a mentioned above. Thus Eqs. (29)-(31) hold for CSM. There exists the parameter region satisfying $a_c = a_c^*$. Using CSM, we can draw the bifurcation diagram and confirm periodic windows corresponding to NBOs in Theorem 1 and to BOs in Proposition 3. However the structure of windows after the crisis is beyond all imagination.

The structure of dynamical ordering in Lemma 1 is similar to those derived in the standard mapping,[12)] the standard–like mappings,[13)] and the forced oscillator.[14)] The dynamical ordering similar to Lemma 1 may hold in the systems possessing the mixed state.

References

1) C. Robinson, *Dynamical Systems* (CRC Press,1999).

2) L. Alsedà, J. Llibre and M. Misiurewicz, *Combinatorial Dynamics and Entropy in Dimension One* (World Scientific, 1993).

3) W. de Melo and S. van Strien, *One–Dimensional Dynamics*, (Springer–Verlag, 1993).

4) T. Horita, H. Hata and H. Mori, Prog. Theor. Phys. **84** (1990), 558.

5) A. Katok, Ergod. Theor. & Dynam. Sys. **2** (1982), 185; G. R. Hall, Ergod. Theor. & Dynam. Sys. **4** (1984), 585.

6) P. Boyland, Contemp. Math. **81** (1988), 119.

7) P. Boyland, Topology and its Appl. **58** (1994), 223.

8) T. Matsuoka, in *Dynamical System* **1** (World Scientific, 1986), p. 58; Contemp. Math. **152** (1993), 229. See also Bussei Kenkyu(Kyoto) **67** (1996), 1.

9) S. Moran, *The Mathematical Theory of Knots and Braids* (North–Holland, 1983).

10) D. Fried, in *Geometric Dynamics.* ed. J. Palis Jr. Lecture Notes in Mathematics **1007** (Springer–Verlag, 1983). p. 261.

11) B. Kolev, C. R. Acad, Sci. Paris, **309**, Ser. I (1989), 835.

12) Y. Yamaguchi and K. Tanikawa (Submitted to Prog. Theor. Phys.).

13) K. Tanikawa and Y. Yamaguchi, *Chaos* **12** (2002), 33.

14) Y. Yamaguchi and K. Tanikawa, Prog. Theor. Phys. **106** (2001), 1097.